

Modulation of Quantum Features of a Driven Two-Level System via a rf Field

Shuning Sun ^{1,*}, Xiangjia Meng ¹, and Xiangji Cai ²

¹ School of Information Engineering, Shandong Youth University of Political Science, Jinan 250103, China; mxj@sdyu.edu.cn

² School of Science, Shandong Jianzhu University, Jinan 250100, China; xiangjicai@foxmail.com

* Correspondence author: shuningsun@sdu.edu.cn

Received date: 3 November 2024; Accepted date: 23 March 2025; Published online: 30 May 2025

Abstract: In this study, we investigated the environmental influences exerted by the rf field on quantum coherence, quantum fidelity and dynamics in a two-level open system. Our results demonstrate that the rf field modulation enables the quantum system to maintain a higher degree of coherence with its initial state within a shorter evolution interval, thereby optimizing evolution speed of the system, suggesting its potential as an additional method for information encoding in quantum communication. By systematically adjusting the rf field modulation index, we observed a notable increase in quantum fidelity, which plays a crucial role in improving the accuracy and stability of quantum computing. Furthermore, the rf field's environmental influence was found to dynamically alter the quantum speed limit (QSL), effectively modulating its tightness. These findings highlight the rf field's capability to optimize the performance of quantum systems, offering new insights for applications in quantum communication, computing and sensing.

Keywords: coherence; fidelity; quantum speed limit

1. Introduction

Quantum communication is an advanced technology that leverages quantum bits (qubits) as information carriers. Qubits are physically realized through quantum systems capable of existing in superposition states. However, in practical quantum communication scenarios, qubits cannot be treated as isolated systems because they inevitably interact with the external environment. These interactions introduce environmental disturbances, leading to the gradual degradation of quantum coherence, which significantly impacts the parallelism and computational efficiency of quantum systems. Moreover, various forms of noise can infiltrate the system, causing unintended state transitions or bit flips and thereby increasing the error rate of quantum computations [1,2]. To enhance the robustness and fault tolerance of quantum computers, a critical focus in the development of quantum information technology is to address these challenges [3,4].

In particular, quantum coherence, fidelity and dynamic evolution of quantum systems are three fundamental factors that profoundly influence the behavior of open quantum systems [1]. The maintenance of quantum coherence is essential for preserving the superposition and entanglement properties of qubits, which are the cornerstones of quantum computing and communication [5]. Decoherence, caused by environmental interactions, directly affects the system's evolution dynamics [3]. Fidelity measures the accuracy of quantum state preservation or transformation. High fidelity ensures that the system evolves as intended, minimizing errors and maximizing computational efficiency. The interplay between coherence and fidelity determines the system's evolution speed and stability [6]. Understanding these dynamics is crucial for designing strategies to mitigate decoherence and noise, thereby accelerating the system's evolution towards the desired state [7]. Therefore, when studying the dynamics of open quantum systems, it is essential to consider these three factors comprehensively. By analyzing and optimizing coherence preservation, fidelity enhancement, and evolution dynamics, more effective quantum control strategies can be developed to enhance the overall performance of quantum systems.

The dynamic evolution of quantum systems over time forms the physical foundation of quantum computing. The speed of evolution in quantum system dynamics reflects to some extent the information transmission rate of the system.

The quantum speed limit (QSL) directly defines the maximum speed at which a quantum system can evolve from the initial state to the target state, and the corresponding shortest time interval is defined as the quantum speed limit time (τ_{QSL}) [8–12]. The quantum speed limit has important application value in quantum communication. For example, precise control and measurement of the evolution speed of quantum systems can improve the operational accuracy and stability of quantum bits, enhance the efficiency and security of key distribution, and thus boost the performance and reliability of quantum computers. By precisely regulating the evolution speed of quantum systems, losses and errors in information transmission can be reduced and communication distances can be extended. Furthermore, the evolution speed of the quantum system can be tailored to meet the specific communication requirements of diverse scenarios and environments.

Recent decades have witnessed many researches on QSL both in closed and open systems [13–29]. In the case of isolated system dynamics, Mandelstam and Tamm originally established the relationship between the minimum evolution time τ_{QSL} from an initial state to an orthogonal state and the energy-time uncertainty $\Delta E(t)$, which is called the the Mandelstam-Tamm (MT) bound [8], i.e., $\tau_{QSL} = \pi\hbar/2\Delta E$. Margolus and Levitin [9] revisited the problem and provided a different bound to the speed of evolution in terms of the difference between the average energy $\langle E(t) \rangle$ and the ground state energy E_0 , i.e., $\tau_{QSL} = \pi\hbar/2(\langle E(t) \rangle - E_0)$, which is called the Margolus-Levitin(ML) bound. The generalization of ML bound from the isolated system to the universal time-dependent (non-)Hermitian quantum system is still under discussion [21,30–35].

In the context of open system dynamics, where energy and/or coherence exchange occurs between the system and its environment, it is necessary to consider general non-unitary quantum evolution. To date, research on the influence of the environment on the quantum speed limit has predominantly focused on non-Markovian dynamic processes. In such cases, it is the non-Markovianity induced by the environment that enhances the evolution speed.

However, when considering a Markovian system, the role of the environment in the memoryless dynamics remains an open question. Specifically, how does the environment interact with and influence the system in the absence of memory effects? Addressing this question is crucial for a comprehensive understanding of quantum dynamics in both Markovian and non-Markovian regimes.

In quantum systems, rf field interacts with quantum states as an external driving field through electromagnetic induction coupling, thereby enabling the control of quantum states. By applying appropriate rf field, the energy uncertainty or the average energy of a quantum system can be increased, which corresponds to the maximum evolution speed defined by the quantum speed limit (QSL). Consequently, the QSL time can be reduced. For example, under the influence of a high-intensity rf field, the rabi oscillation frequency increases, accelerating the evolution of quantum states. Therefore, rf field plays a modulation role in driving quantum systems toward the quantum speed limit. RF field can also alter the energy level structure of quantum systems, optimizing the transition paths between quantum states. By tuning the parameters of the rf field, more efficient quantum state evolution can be achieved for further approaching the QSL. In practical quantum systems, decoherence effects can impact the evolution speed of quantum states. RF field can suppress decoherence effects through techniques such as dynamical decoupling, allowing the quantum system to evolve closer to the QSL. In recent years, numerous works have validated the effectiveness of rf field in modulating the dynamics of quantum systems. For instance, in superconducting qubit systems, rf field is widely used to achieve rapid quantum state manipulation [36,37]. By optimizing rf pulse sequences, researchers have successfully realized quantum state evolution approaching the QSL [11,38,39]. In ion-trap quantum computing, rf field is employed to drive transitions between internal and motional states of ions [40,41]. In solid-state spin systems, rf field is utilized to manipulate electron spin states [42,43]. In certain quantum systems, such as two-level systems, driven qubits, nuclear magnetic resonance (NMR) systems, and quantum sensing platforms, the interaction between the rf field and the quantum system leads to dynamic processes that can be effectively described within the Markovian approximation. This approximation assumes that the system's evolution depends solely on its current state, without memory effects from its past history.

Inspired by these foundational insights, in this work, we employ the widely utilized two-level system as the fundamental framework for our investigation [44–48]. The system's dynamics are governed by a dynamical semigroup, with its evolution described by a Lindblad master equation [49–51]. The Hamiltonian of the system is driven by both laser field and rf field, where the laser field facilitates the transition from a lower to a higher energy state by providing momentum, while the rf field acts as an environmental influence. Our study primarily explores the modulation effects of the rf field—representing environmental interactions—on quantum coherence, quantum fidelity and the quantum speed limit, demonstrating the beneficial role of environmental influences in enhancing quantum information

processing. The paper is organized as follows. In Section 2, we present our model and theoretical framework. In Section 3, we give the numerical results and discussion. In Section 4, we give a brief conclusion.

2. Theoretical Framework

2.1. Modulation of a Driven Two-Level System via a rf Field

Building up a single molecule model with two discrete nondegenerate states, the ground state $|g\rangle$ and the excited state $|e\rangle$, separated by $\Delta E = \hbar\omega_0(t)$ ($\omega_0(t)$ is the transition frequency). When the Hamiltonian of this two-level system is driven by laser and rf fields simultaneously. After adopting a rotating wave approximation for the laser field, the time-dependent Hamiltonian is defined as [52,53]

$$\hat{\mathcal{H}}(t) = \frac{1}{2}\delta(t)\sigma_z + \frac{1}{2}\Omega\sigma_x, \quad (1)$$

where $\delta(t)$ is defined as a general detuning frequency, $\delta(t) = \delta_L - \Omega_{rf}(t)$. δ_L is the static detuning between incident laser field frequency and inner atomic frequency, $\delta_L = \omega_0 - \omega_L$. ω_L is the laser field frequency and ω_0 is the transition frequency. Taking no account of the diffusion spectrum, ω_0 is defined as a constant. Ω is the laser Rabi frequency. Considering the laser field is a continuous field, so $\Omega = \text{constant}$. $\Omega_{rf}(t)$ is the time-dependent rf field Rabi frequency and $\Omega_{rf}(t) = \zeta\omega_{rf}\cos(\omega_{rf}t)$. ζ is the rf field modulation, ω_{rf} is rf field frequency.

The dynamics of the two-level system is ruled by a Markovian master equation,

$$\mathbb{L}\rho_t = -\frac{i}{\hbar}[\hat{\mathcal{H}}(t), \rho_t] + \sum_k \left(\hat{F}_k \rho(t) \hat{F}_k^\dagger - \frac{1}{2} \{ \hat{F}_k^\dagger \hat{F}_k, \rho(t) \} \right). \quad (2)$$

Eq. (2) is the GKLS (Gorini Kosakowski Lindblad Sudarshan) equation for the evolution of open quantum systems. Its form was first proposed by Gorini, Kossakowski, and Sudarshan in their 1976 paper [49], and further extended and formalized by Lindblad in the same year's work [50]. Here \mathbb{L} is defined as the Lindblad operator, ρ_t is the evolution density matrix of the system, $\hat{\mathcal{H}}(t)$ is the Hamiltonian of system, \hat{F}_k is the operator of environmental dissipation, $\hat{F}_k = \sqrt{\Gamma_k} \begin{pmatrix} 0 & 0 \\ 1 & 0 \end{pmatrix}$, Γ is the spontaneous emission rate. In a two-level system, $k = 1$.

The evolution of the density matrix under such a two-level system Hamiltonian is given by the solution of Liouville equation $\frac{d\rho_t}{dt} = \mathbb{L}\rho_t$,

$$\begin{aligned} \dot{\rho}_{ee} &= \frac{i}{2}\Omega(\rho_{eg} - \rho_{ge}) - \Gamma\rho_{ee} \\ \dot{\rho}_{gg} &= -\frac{i}{2}\Omega(\rho_{eg} - \rho_{ge}) + \Gamma\rho_{ee} \\ \dot{\rho}_{ge} &= \frac{i}{2}\Omega(\rho_{gg} - \rho_{ee}) - i\delta(t)\rho_{ge} - \frac{\Gamma}{2}\rho_{ge} \\ \dot{\rho}_{eg} &= -\frac{i}{2}\Omega(\rho_{gg} - \rho_{ee}) + i\delta(t)\rho_{eg} - \frac{\Gamma}{2}\rho_{eg}. \end{aligned} \quad (3)$$

The evolved density matrix at any time can be obtained from Eq. (3), and the form can be generally represented by $\rho_t = \begin{pmatrix} \rho_{ee} & \rho_{eg} \\ \rho_{ge} & \rho_{gg} \end{pmatrix}$, where ρ_{ee} , ρ_{eg} , ρ_{ge} and ρ_{gg} are all time-dependent.

With the introduction of Bloch vectors,

$$\mathcal{U} = \frac{1}{2}(\rho_{ge} + \rho_{eg}), \mathcal{V} = \frac{1}{2i}(\rho_{ge} - \rho_{eg}), \mathcal{W} = \frac{1}{2}(\rho_{ee} - \rho_{gg})$$

(\mathcal{U} , \mathcal{V} and \mathcal{W} are simplified forms of $\rho_{ge}(t)$, $\rho_{eg}(t)$ and $\rho_{ee}(t) - \rho_{gg}(t)$). Eq. (3) can be rewritten as the functions of \mathcal{U} , \mathcal{V} , \mathcal{W}

$$\begin{aligned}
\dot{\mathcal{U}} &= \delta(t)\mathcal{V} - \frac{\Gamma}{2}\mathcal{U} \\
\dot{\mathcal{V}} &= -\Omega\mathcal{W} - \delta(t)\mathcal{U} - \frac{\Gamma}{2}\mathcal{V} \\
\dot{\mathcal{W}} &= \Omega\mathcal{V} - \Gamma\mathcal{W} - \frac{\Gamma}{2}.
\end{aligned} \tag{4}$$

2.2. Some Quantum Features of Open Quantum Systems

In an open quantum system, interactions with the surrounding environment are inevitable, resulting in noise and disturbances that can significantly impact the system's coherence. These environmental interactions typically cause a gradual and often irreversible loss of coherence, a phenomenon known as decoherence, which accumulates over time. A prominent example of this issue arises in the field of quantum computing, where the interaction between qubits and their environment can lead to the decoherence of quantum states. This decoherence process poses a fundamental challenge to the feasibility and reliability of quantum computing, as it directly affects the stability and fidelity of quantum operations. The fidelity of quantum operations, which measures the accuracy of a quantum state or process compared to its ideal form, is particularly sensitive to decoherence. Moreover, decoherence alters the quantum dynamics of the system, disrupting phenomena such as quantum superposition and entanglement, which are essential for quantum information processing. Therefore, understanding and mitigating decoherence, while preserving the fidelity and quantum dynamics of the system, is crucial for advancing practical quantum technologies.

2.2.1. Quantum Coherence

In quantum information processing, the quantum coherence is one of the key factors for realizing tasks such as quantum computing and quantum communication. The coherence norm is defined as

$$C(\rho) = \sum_{i \neq j} |\rho_{ij}|, \tag{5}$$

where ρ_{ij} represents the matrix elements under a specific basis. Quantum coherence enables interference effects between quantum states, thereby accelerating the evolution of the system. When the system is subjected to environmental noise or decoherence effects, the decay of coherence leads to a slowdown in the evolution speed, consequently prolonging the time required to reach the target state. By analyzing coherence, optimized control strategies (such as dynamical decoupling or quantum error correction) can be designed to protect coherence, thus reducing the evolution time. In quantum control, through the analysis of coherence, more precise control pulses can be designed, thereby approaching the quantum speed limit [54–57].

2.2.2. Fidelity

The fidelity between the evolved density matrix ρ_t and the initial density matrix ρ_0 is defined as

$$F_b(\rho_0, \rho_t) = \text{Tr} \sqrt{\sqrt{\rho_0} \rho_t \sqrt{\rho_0}}. \tag{6}$$

Fidelity provides a standardized method for measuring the similarity between a quantum state and its target state, thereby offering a quantitative basis for calculating the quantum speed limit. By studying the variation of fidelity over time, one can derive the minimum time required for the evolution of a quantum state [58–62]. In practical quantum systems, environmental noise and decoherence effects cause the quantum state to deviate from the ideal evolution path. The changes in fidelity directly reflect the impact of these disturbances on the system's evolution, thereby providing critical information for the study of quantum speed limits. By analyzing the relationship between fidelity and speed limits, more efficient quantum control strategies can be designed to reduce evolution time and enhance the robustness of the system. Fidelity is a physically measurable quantity. By experimentally determining fidelity, it is possible to indirectly validate theoretical predictions of the quantum speed limit, thus offering guidance for experimental design. In quantum computing and quantum communication, fidelity is a key parameter for evaluating the quality of quantum gate operations and quantum state transmission.

2.2.3. Quantum Speed Limit

To derive the Quantum Speed Limit (QSL) for a quantum system evolving from the initial state ρ_0 to the final state ρ_t , it is essential to select an appropriate metric, such as fidelity, to quantify the distance between these two states. Using a specific metric $\mathcal{L} \equiv \mathcal{L}(\rho_0, \rho_t)$, we can construct the geodesic line connecting ρ_0 and ρ_t . This geodesic represents the shortest possible path between the two states in the given metric space. The QSL is generally defined as the lower bound of the evolution time τ_{QSL} , which can be derived based on an integral inequality related to the system's dynamics and the chosen metric [11,32,63].

$$\left| \int_0^\tau \dot{\mathcal{L}} dt \right| \leq \int_0^\tau |\dot{\mathcal{L}}| dt, \quad (7)$$

which gives

$$\tau \geq \tau_{\text{QSL}} = \frac{\left| \int_0^\tau \dot{\mathcal{L}} dt \right|}{\frac{1}{\tau} \int_0^\tau |\dot{\mathcal{L}}| dt}, \quad (8)$$

where $\ell = \int_0^\tau |\dot{\mathcal{L}}| dt$ is defined as the length of the evolution path. $v_{\text{QSL}} = |\dot{\mathcal{L}}| \equiv \left| \frac{d\mathcal{L}}{dt} \right|$ is employed to define the maximum evolution speed. Researches have shown that the changing rate of geodesic is closely related to both the energy distribution of the system and the changing rate of the geometric path traversed by a quantum state during its evolution in Hilbert space [32,33,35]. This approach establishes a fundamental limit on the minimum time required for a quantum system to transition between two states, providing critical insights into the dynamics and efficiency of quantum processes.

In this work, we choose the Fubini-Study metric to define the length of geodesic as $\mathcal{L} = \arccos \left[\text{Tr} \sqrt{\rho(0)\rho(t)} \right]$. Previous work has verified that under such a metric, the maximum evolution speed in open system can be calculated as [11,32]

$$v_{\text{QSL}} = \|\mathbb{L}\rho_t\| = \sqrt{\text{Tr}(\mathbb{L}\rho_t)^2}. \quad (9)$$

From Eq. (3) and Eq. (9), the relationship between v_{QSL} and the quantum coherence can also be established.

3. Numerical Results and Discussion

Figure 1 shows line shapes of the coherence norm $\mathcal{C}(\rho)$ as functions of the scaled evolution time Γt . When $\xi = 0$ (denoted in solid red line), the coherence norm $\mathcal{C}(\rho)$ tends to a stable value after a prolonged scaled evolution time Γt . This behavior can be attributed to the laser field's ability to induce electronic transitions in the two-level system. As the evolution time increases, the system gradually approaches a stable quantum state distribution under the influence of the laser field, causing the coherence norm $\mathcal{C}(\rho)$ to stabilize at a constant value. When both the rf field and the laser field are applied to a quantum system, intricate and multifaceted coupling effects can emerge. The key role of the laser field lies in driving quantum transitions within a two-level system, thereby facilitating the formation of coherent superposition states. The introduction of a rf field modulates the interaction between the laser field and the system. As shown in Figure 1, the periodic oscillation of the rf field occurs on a short time scale, and the rf field can induce transitions between two energy levels in the quantum system, leading to periodic evolution of the quantum state. Therefore, it causes coherence oscillations in quantum systems in a short period of time. However, by optimizing design, such as dynamic decoupling, coherence enhancement can be achieved over a long time scale [64–66].

The manuscript explores the quantum speed limit (QSL) by examining the dynamic behavior of quantum systems over short time intervals. As illustrated in Figure 1, enhancing ξ enables the quantum system to maintain a higher degree of coherence with its initial state within a shorter evolution interval, which means the evolution speed of the system has also been optimized, thereby increasing the quantum speed limit. The improvement of quantum speed limit thus not only increases computational throughput and communication efficiency but also strengthens the resilience of quantum systems against noise and errors, paving the way for more practical and scalable quantum technologies.

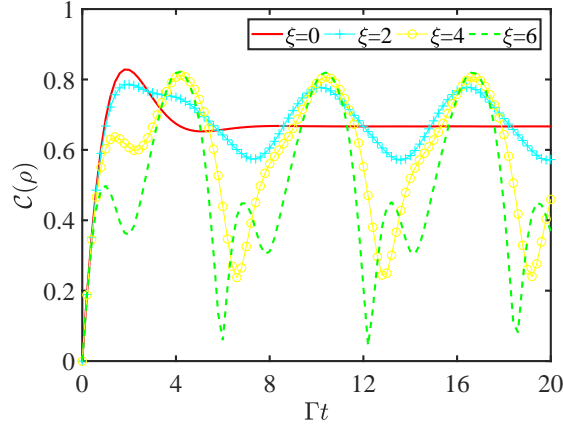


Figure 1. Line shapes of the coherence norm $\mathcal{C}(\rho) = \sum_{i \neq j} |\rho_{ij}|$ (ρ_{ij} is the matrix elements under a specific basis) as functions of the scaled evolution time Γt . Parameters used include, $\Omega = \Gamma$, $\omega_{rf} = 0.5\Gamma$, $\delta_L = 0$ and $\Gamma = 20$ MHz. $\zeta = 0$ (denoted in solid red line), $\zeta = 2$ (denoted in the ‘+’ marked cyan line), $\zeta = 4$ (denoted in the ‘o’ marked yellow line) and $\zeta = 6$ (denoted in dashed green line). The ground state is chosen as the initial state $\mathcal{W}(0) = -1/2$.

The fidelity between the evolved density matrix ρ_t and the initial density matrix ρ_0 is defined as $F_b(\rho_0, \rho_t)$ in Eq. (6) with ρ_0 being a diagonal matrix at $\mathcal{W}(0) = -1/2$. Figure 2 shows line shapes of the fidelity F_b as functions of the scaled evolution time Γt . When the rf modulation index $\zeta = 0$, the fidelity F_b exhibits a gradual decline from its initial value $F_b(\rho_0, \rho_0) = 1$, ultimately converging to a stable value over the course of time evolution. This stabilization of quantum fidelity is likely attributed to several factors: the system achieving a steady state, the establishment of an equilibrium in the interaction between the laser field and the system, and the progressive diminishment of the impact of decoherence.

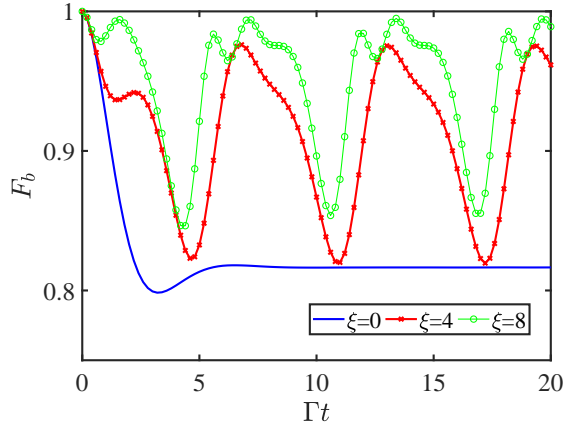


Figure 2. Line shapes of the fidelity F_b as functions of the scaled evolution time Γt . Parameters used include, $\Omega = \Gamma$, $\omega_{rf} = 0.5\Gamma$, $\delta_L = 0$ and $\Gamma = 20$ MHz. $\zeta = 0$ (the solid blue line), $\zeta = 4$ (the ‘x’ marked red line) and $\zeta = 8$ (the ‘o’ marked green line). The ground state is chosen as the initial state $\mathcal{W}(0) = -1/2$.

When the rf field is introduced into the system, it induces changes on the fidelity F_b of quantum systems (the line shapes of the ‘x’ marked red line and the ‘o’ marked green line in Figure 2). As the intensity of the rf field varies periodically, this variation can lead to changes in the transition probability and energy level occupation of particles in the quantum system, causing the quantum fidelity oscillating with time. As the rf modulation index increases, the strength of its interaction with the quantum system also increases. The rf field can more effectively couple different energy levels and facilitate the transition of particles between these energy levels. This enhanced coupling can improve the precision of quantum states manipulation, thereby increasing quantum fidelity. Improving the fidelity of quantum system is of great significance in quantum information research, and it can enhance the accuracy and

stability of quantum computing, reduce computational errors, and improve the reliability and range of quantum information transmission.

In the following, we demonstrate the rf modulation index of ζ on the evolution speed of quantum systems. Taking Figure 3 as an instance, the feasible time τ_{ζ} at which the evolved state $\rho(\tau_{\zeta})$ arrives at the largest distance \mathcal{L}^{max} from the initial state $\rho(0)$ for the first time, depends on the rf modulation index ζ . In the following, our discussions will be conducted within the time range of 0 to τ_{ζ} where τ_{ζ} is determined by \mathcal{L}^{max} under parameter ζ .

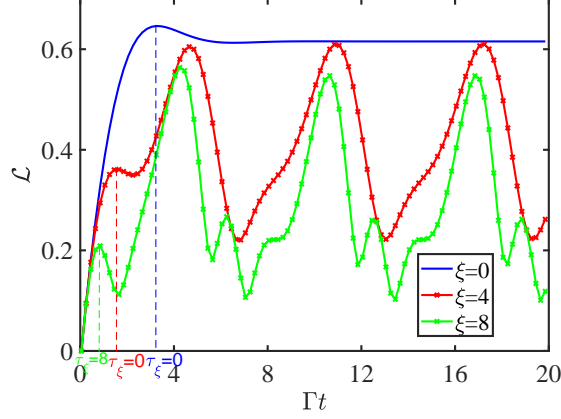


Figure 3. The length of geodesic \mathcal{L} as functions of the scaled evolution time Γt under varied rf field modulation index ζ . Parameters used include, $\Omega = \Gamma$, $\omega_{rf} = 0.5\Gamma$, $\delta_L = 0$ and $\Gamma = 20$ MHz. $\zeta = 0$ (the solid blue line), $\zeta = 4$ (the ‘x’ marked red line) and $\zeta = 8$ (the ‘o’ marked green line). The ground state is chosen as the initial state $\mathcal{W}(0) = -1/2$.

In Figure 4a, we discussed the geodesic length \mathcal{L} as functions of Γt under varied rf field modulation index ζ . The time τ_{ζ} that required to reach the largest distance \mathcal{L}^{max} from the initial state $\rho(0)$ decreases with increasing rf field modulation index ζ . In Figure 4b, we find that increasing ζ can also obtain higher v_{QSL} at τ_{ζ} . Figure 4c shows the ratio of the quantum speed limits time τ_{QSL} to the actual evolution time τ , τ_{QSL}/τ , which also can be defined as the tightness of quantum speed limits. As shown in Figure 4c, the tightness decreases with the scaled evolution time, which means higher potential for speeding up a quantum system increases.

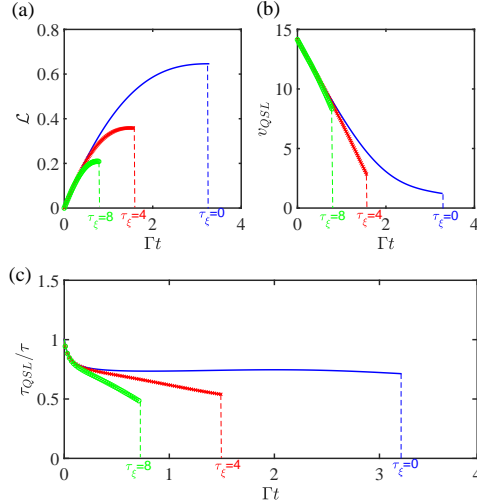


Figure 4. (a) The length of the geodesic \mathcal{L} as functions of Γt under varied rf field modulation index ζ . Γt ranges from 0 to τ_{ζ} . τ_{ζ} is determined by the the first time for \mathcal{L} reaches the maximum value \mathcal{L}^{max} . (b) The maximum evolution speed v_{QSL} as functions of Γt under varied rf field modulation index ζ . (c) τ_{QSL}/τ as functions of Γt under varied rf field modulation index ζ . Parameters used include, $\Omega = \Gamma$, $\omega_{rf} = 0.5\Gamma$, $\delta_L = 0$ and $\Gamma = 20$ MHz. $\zeta = 0$ (the solid blue line), $\zeta = 4$ (the ‘x’ marked red line) and $\zeta = 8$ (the ‘o’ marked green line). The ground state is chosen as the initial state $\mathcal{W}(0) = -1/2$.

Figure 5 illustrates the variation of τ_{QSL}/τ as function of the rf modulation index ζ . We selected the τ_{QSL}/τ corresponding to τ_{ζ} under each value of ζ . The result shows that the rf field can not only modulate the tightness the quantum speed limit bound at specific index ζ ($\zeta \simeq 3.4$ in Figure 5), which can be attributed to the collective influence of various factors, including quantum geometric effects, resonance effects, and quantum phase transitions, but also reduce the tightness within the entire range of ζ , which is consistent with the conclusion in Figure 4b, meaning an increase of evolution speed v_{QSL} . The tightness of the quantum speed limit can significantly influence the response speed and measurement accuracy of quantum sensors.

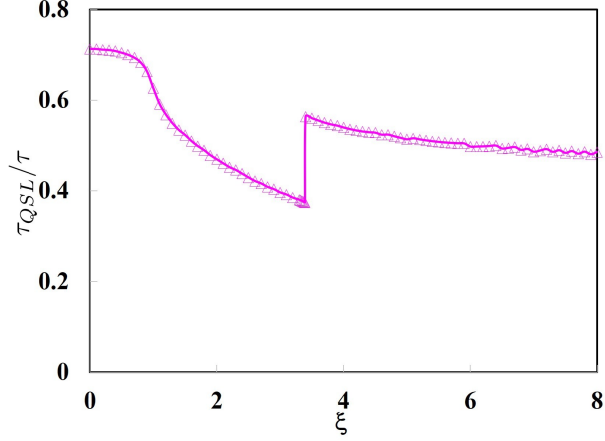


Figure 5. The τ_{QSL}/τ as function of the rf modulation index ζ . Parameters used include, $\Omega = \Gamma$, $\omega_{rf} = 0.5\Gamma$, $\delta_L = 0$ and $\Gamma = 20$ MHz. The ground state is chosen as the initial state $\mathcal{W}(0) = -1/2$.

We also discuss the maximum fidelity when the length of the geodesic reaches the largest \mathcal{L}^{max} for the first time at τ_{ζ} under different ζ . The results are shown in Figure 6.

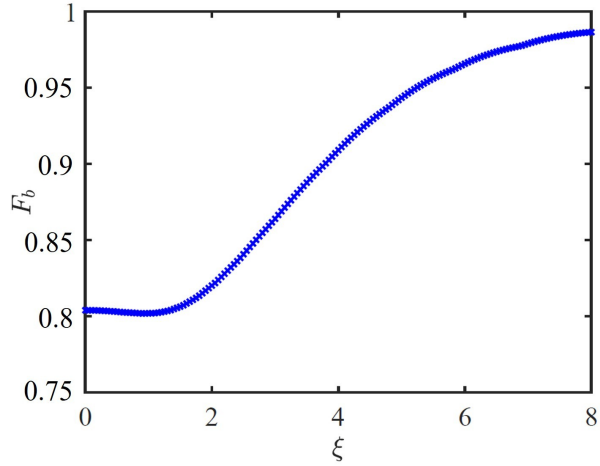


Figure 6. The fidelity F_b between the evolved density matrix $\rho_{\tau_{\zeta}}$ and the initial density matrix ρ_0 as function of the rf modulation index ζ . Parameters used include, $\Omega = \Gamma$, $\omega_{rf} = 0.5\Gamma$, $\delta_L = 0$ and $\Gamma = 20$ MHz. The ground state is chosen as the initial state $\mathcal{W}(0) = -1/2$.

Figure 6 illustrates the maximum fidelity F_b between the evolved density matrix $\rho_{\tau_{\zeta}}$ and the initial density matrix ρ_0 as function of the rf modulation index ζ . As shown in the figure, we observe that the rf modulation ζ can effectively modulate the maximum fidelity F_b . Moreover, as the rf modulation ζ increases, the maximum fidelity F_b generally increases. By increasing ζ , the anti-interference ability of quantum communication systems can be improved, enabling more stable transmission of quantum signals under adverse conditions such as environmental noise and interference, thereby reducing the likelihood of communication errors and interruptions.

4. Conclusion

In this work, we investigated the quantum coherence, fidelity and quantum speed limits in a two-level open system in a two-level open system driven simultaneously by a laser field and a rf field or excited solely by a laser field. Compared to the case where quantum coherence tends to stabilize under the sole driving of the laser field, the combined action of the laser and rf fields results in periodic oscillations in coherence. In quantum communication, modulating the quantum coherence through the rf field modulation can serve as an additional method for information encoding, thereby improving the efficiency and security of quantum communication.

We studied the fidelity between the evolved density matrix and the initial density matrix. Under the sole driving of the laser field, fidelity decreases from its initial value and eventually stabilizes over time. However, when the rf field is introduced into the system, quantum fidelity oscillates over time and increases with the rf modulation index. Improving the fidelity of quantum system is of great significance to quantum information research, as it can improve the accuracy and stability of quantum computing, reduce calculation errors, improve the reliability of quantum information transmission and expand the transmission range.

We also investigated the quantum speed limits in the two-level open system. Our work begins with the evolution starting from the ground initial state. We observed that the environmental influence, characterized by rf field modulation index, can increase the potential for enhancing the evolution speed of quantum system and modulate the tightness of the quantum speed limit. In quantum information, this property can serve as an indicator for evaluating the efficiency of different quantum computing schemes, achieving faster communication speed and higher security, while also influencing the response speed and measurement accuracy of quantum sensors.

Furthermore, many intriguing results remain to be explored in depth. For instance, the quantum dynamical behavior under different combinations of field strengths, the characteristics of quantum speed limits in more complex environments, and the practical application potential of these findings in quantum technologies. These studies will provide new theoretical support and experimental guidance for the advancement of quantum information science.

Author Contributions

Shuning Sun: Conceptualization (equal); Formal analysis (equal); Investigation (equal); Writing—original draft (equal); Writing—review & editing (equal). Xiangjia Meng: Formal analysis (equal); Investigation (equal); Writing—review & editing (equal). Xiangji Cai: Conceptualization (supporting); Formal analysis (equal); Investigation (equal); Writing—review & editing (equal). All authors have read and agreed to the published version of the manuscript

Funding

The work was supported by the National Natural Science Foundation of China (Grant No. 12204277) and Shandong Province Natural Science Foundation (Grant No. ZR2024QA025).

Conflicts of Interest

The authors have no conflicts to disclose.

Data Availability Statement

The data that support the findings of this study are available from the corresponding author upon reasonable request.

Acknowledgments

We thank the National Natural Science Foundation of China (Grant No. 12204277) and Shandong Province Natural Science Foundation (Grant No. ZR2024QA025).

References

1. J. Preskill, Quantum Computing in the NISQ era and beyond. *Quantum* (2018).
2. J. Biamonte, P. Wittek, N. Pancotti, P. Rebentrost, N. Wiebe, and S. Lloyd, Quantum machine learning. *Quantum* (2017).
3. B. M. Terhal, Quantum error correction for quantum memories. *Rev. Mod. Phys.* **87**, 307 (2015).
4. M. A. Khan, S. Ghafoor, S. M. H. Zaidi, H. Khan, and A. Ahmad, From quantum communication fundamentals to decoherence mitigation strategies: Addressing global quantum network challenges and projected applications. *Heliyon* **10**, e34331 (2024).
5. M. A. Nielsen and I. L. Chuang, *Quantum Computation and Quantum Information: 10th Anniversary Edition* (Cambridge University Press: Cambridge, UK, 2010).
6. V. Giovannetti, S. Lloyd, and L. Maccone, Quantum-Enhanced Measurements: Beating the Standard Quantum Limit. *Science* **306**, 1330 (2004).

7. Z. Cai, R. Babbush, S. C. Benjamin, S. Endo, W. J. Huggins, Y. Li, J. R. McClean, and T. E. O'Brien, Quantum error mitigation. *Rev. Mod. Phys.* **95**, 045005 (2023).
8. L. Mandelstam and I. Tamm, The Uncertainty Relation Between Energy and Time in Non-relativistic Quantum Mechanics. In: Bolotovskii, B.M., Frenkel, V.Y., Peierls, R. (eds) *Selected Papers*. Springer, Berlin, Heidelberg, 1991, pp. 115–123.
9. N. Margolus and L. B. Levitin, The maximum speed of dynamical evolution. *Physica D* **120**, 188 (1998).
10. L. B. Levitin and T. Toffoli, Fundamental Limit on the Rate of Quantum Dynamics: The Unified Bound Is Tight. *Phys. Rev. Lett.* **103**, 160502 (2009).
11. A. del Campo, I. L. Egusquiza, M. B. Plenio, and S. F. Huelga, Quantum Speed Limits in Open System Dynamics. *Phys. Rev. Lett.* **110**, 050403 (2013).
12. Y. Zhang, W. Han, Y. Xia, J. Cao, and H. Fan, Quantum speed limit for arbitrary initial states. *Sci. Rep.* **4**, 4890 (2014).
13. Y. Wu, J. Yuan, C. Zhang, Z. Zhu, J. Deng, X. Zhang, P. Zhang, Q. Guo, Z. Wang, J. Huang, C. Song, H. Li, D.-W. Wang, H. Wang, and G. S. Agarwal, Testing the unified bounds of the quantum speed limit. *Phys. Rev. A* **110**, 042215 (2024).
14. K. Bhattacharyya, Quantum decay and the Mandelstam-Tamm-energy inequality. *J. Phys. A* **16**, 2993 (1983).
15. B. Yadin, S. Imai, and O. Gühne, Quantum Speed Limit for States and Observables of Perturbed Open Systems. *Phys. Rev. Lett.* **132**, 230404 (2024).
16. Z.-y. Mai and C.-s. Yu, Tight and attainable quantum speed limit for open systems. *Phys. Rev. A* **108**, 052207 (2023).
17. K. Kobayashi, Reachable-set characterization of an open quantum system by the quantum speed limit. *Phys. Rev. A* **105**, 042608 (2022).
18. S.-S. Nie, F.-H. Ren, R.-H. He, J. Wu, and Z.-M. Wang, Control cost and quantum speed limit time in controlled almost-exact state transmission in open systems. *Phys. Rev. A* **104**, 052424 (2021).
19. A. J. B. Rosal, D. O. Soares-Pinto, and D. P. Pires, Quantum speed limits based on Schatten norms: Universality and tightness. *Phys. Lett. A* **534** (2025).
20. T. Nishiyama and Y. Hasegawa, Speed limits and thermodynamic uncertainty relations for quantum systems with the non-Hermitian Hamiltonian. *Phys. Rev. A* **111**, 012214 (2025).
21. V. Giovannetti, S. Lloyd, and L. Maccone, Quantum limits to dynamical evolution. *Phys. Rev. A* **67**, 052109 (2003).
22. J. Anandan and Y. Aharonov, Geometry of quantum evolution. *Phys. Rev. Lett.* **65**, 1697 (1990).
23. I. Brouzos, A. I. Streltsov, A. Negretti, R. S. Said, T. Caneva, S. Montangero, and T. Calarco, Quantum speed limit and optimal control of many-boson dynamics. *Phys. Rev. A* **92**, 062110 (2015).
24. Z. Hu, L. Wang, H. Chen, H. Yuan, C.-H. F. Fung, J. Liu, and Z. Miao, Tight bounds of quantum speed limit for noisy dynamics via maximal rotation angles. (2023), arXiv:1601.00150 .
25. A. Steane, C. F. Roos, D. Stevens, A. Mundt, D. Leibfried, F. Schmidt-Kaler, and R. Blatt, Speed of ion-trap quantum-information processors. *Phys. Rev. A* **62**, 042305 (2000).
26. J. J. García-Ripoll, P. Zoller, and J. I. Cirac, Speed Optimized Two-Qubit Gates with Laser Coherent Control Techniques for Ion Trap Quantum Computing. *Phys. Rev. Lett.* **91**, 157901 (2003).
27. P. Lu, T. Liu, Y. Liu, X. Rao, Q. Lao, H. Wu, F. Zhu, and L. Luo, Realizing quantum speed limit in open system with a π -symmetric trapped-ion qubit. *New J. Phys.* **26**, 013043 (2024).
28. M. Musadiq, Quantum Speed Limit Time of A Spin Qubit Coupled With Heisenberg Spin Environment. *Int. J. Theor. Phys.* **63**, 205 (2024).
29. M. Musadiq, S. Khan, M. Javed, and M. Shamirzaie, Quantum speed limit time of a spin qubit in noninteracting spin bath. *Int. J. Quant. Inf.* **17**, 1950054 (2019).
30. P. J. Jones and P. Kok, Geometric derivation of the quantum speed limit. *Phys. Rev. A* **82**, 022107 (2010).
31. M. Zwiernik, Comment on “Geometric derivation of the quantum speed limit”. *Phys. Rev. A* **86**, 016101 (2012).
32. S. Deffner and E. Lutz, Quantum Speed Limit for Non-Markovian Dynamics. *Phys. Rev. Lett.* **111**, 010402 (2013).
33. S. Deffner and E. Lutz, Energy–time uncertainty relation for driven quantum systems. *J. Phys. A* **46**, 335302 (2013).
34. M. Okuyama and M. Ohzeki, Comment on ‘Energy-time uncertainty relation for driven quantum systems’. *J. Phys. A* **51**, 318001 (2018).

35. S. Sun, Y. Peng, X. Hu, and Y. Zheng, Quantum Speed Limit Quantified by the Changing Rate of Phase. *Phys. Rev. Lett.* **127**, 100404 (2021).
36. V. Chouhan, T. Ring, G. Wu, and E. Viklund, Mitigation of Pitting on Nitrogen-Doped Niobium Surfaces through Two-Step Electropolishing. *J. Electrochem. Soc.* **172**, 023502 (2025).
37. T. Zhu, X. Bao, Y. He, Z. Xue, Y. Qiu, C. Li, W. Xue, T. Jiang, Q. Chu, H. Guo, S. Huang, Z. Yang, W. Yue, J. Chen, M. Xu, S. Zhang, K. Zhang, H. Zhao, T. Tan, and A. Wu, Plasma characterization and modulation techniques for 1.3 GHz, 9-cell superconducting rf cavity cleaning. *Phys. Rev. Accel. Beams* **27**, 123101 (2024).
38. J. Slim, N. N. Nikolaev, F. Rathmann, A. Wirzba, A. Nass, V. Hejny, J. Pretz, H. Soltner, F. Abusaif, A. Aggarwal, A. Aksentev, A. Andres, L. Barion, G. Ciullo, S. Dymov, R. Gebel, M. Gaisser, K. Grigoryev, D. Grzonka, O. Javakhishvili, A. Kacharava, V. Kamerdzhev, S. Karanth, I. Keshelashvili, A. Lehrach, P. Lenisa, N. Lomidze, B. Lorentz, A. Magiera, D. Mchedlishvili, F. Müller, A. Pesce, V. Poncza, D. Prasuhn, A. Saleev, V. Shmakova, H. Ströher, M. Tabidze, G. Tagliente, Y. Valdau, T. Wagner, C. Weidemann, A. Wrońska, and M. Żurek (JEDI Collaboration), First detection of collective oscillations of a stored deuteron beam with an amplitude close to the quantum limit. *Phys. Rev. Accel. Beams* **24**, 124601 (2021).
39. S. Vappangi, T. Deepa, V. Mani, and N. Bharathiraja, On the performance of delta sigma modulators for DCO-OFDM based NOMA visible light communication systems. *Opt. Laser Technol.* **167**, 109653 (2023).
40. F. Ni, Z. Song, J. Chen, B. Xu, F. Xu, and L. Ding, Achieving Electron Capture Dissociation in the Radio Frequency Linear Ion Trap without the Assistance of a Magnetic Field A Simulation Study. *J. Am. Soc. Mass Spectrom.* **35**, 2499 (2024).
41. J.-Y. Wang, W.-X. Huang, Y.-L. Tian, Y.-S. Wang, Y. Wang, W.-L. Zhang, Y.-J. Huang, Z.-G. Gan, and H.-S. Xu, A Radio-Frequency Ion Trap System for the Multi-Reflection Time-of-Flight Mass Spectrometer at SHANS and Its Offline Commissioning. *Atoms* **11** (2023).
42. D. J. Sorce and S. Michaeli, On the geometric phase effects on time evolution of the density matrix during modulated radiofrequency pulses. *J. Magn. Reson.* **372**, 107840 (2025).
43. C. Hao, Z. Qiu, Q. Sun, Y. Zhu, and D. Sheng, Interactions between nonresonant rf fields and atoms with strong spin-exchange collisions. *Phys. Rev. A* **99**, 053417 (2019).
44. C. Cohen-Tannoudji, J. Dupont-Roc, and G. Grynberg, *Atom—Photon Interactions: Basic Process and Applications* (Wiley-VCH Verlag GmbH, 2008).
45. P. Poggi, F. Lombardo, and D. Wisniacki, Quantum speed limit and optimal evolution time in a two-level system. *Europhys. Lett.* **104**, 40005 (2013).
46. G. C. Hegerfeldt, Driving at the Quantum Speed Limit: Optimal Control of a Two-Level System. *Phys. Rev. Lett.* **111**, 260501 (2013).
47. Y. Zheng and F. L. H. Brown, Single-Molecule Photon Counting Statistics via Generalized Optical Bloch Equations. *Phys. Rev. Lett.* **90**, 238305 (2003).
48. Y. Zhang, W. Han, Y. Xia, J. Cao, and H. Fan, Classical-driving-assisted quantum speed-up. *Phys. Rev. A* **91**, 032112 (2015).
49. V. Gorini, A. Kossakowski, and E. C. G. Sudarshan, Completely positive dynamical semigroups of N-level systems. *J. Math. Phys.* **17**, 821 (1976).
50. G. Lindblad, On the generators of quantum dynamical semigroups. *Commun. Math. Phys.* **48**, 119 (1976).
51. G. C. Ghirardi, P. Pearle, and A. Rimini, Markov processes in Hilbert space and continuous spontaneous localization of systems of identical particles. *Phys. Rev. A* **42**, 78 (1990).
52. F. Shikerman, L. P. Horwitz, and A. Pe'er, Reconstruction of the environmental correlation function from single-emitter photon statistics: A non-Markovian approach. *Phys. Rev. A* **87**, 053851 (2013).
53. F. Shikerman and E. Barkai, Probing dynamics of single molecules: Nonlinear spectroscopy approach. *J. Chem. Phys.* **129**, 244702 (2008).
54. S. Mouslih, Z. Dahbi, M. Jakha, S. El Asri, S. Taj, and B. Manaut, Influence of an external electromagnetic field on quantum entanglement and coherence in a two-qubit graphene system. *Phys. Scr.* **100**, 035104 (2025).
55. H. Sun, H. Chen, J. Ma, W. Tao, M. Liu, and X. Yang, Protecting quantum coherence of semiconductor qubit by utilizing charge noise. *Laser Phys. Lett.* **22**, 035201 (2025).
56. N.-N. Zhang, C.-Y. Wu, X. Zhou, Q.-Y. Liu, C.-G. Liu, Y.-R. Guo, and R.-P. Li, Tunable non-Markovian and quantum coherence in the single-qubit dephasing noise channel. *Sci. China Phys. Mech. Astron.* **68**, 230313 (2025).

57. A. Garg and A. K. Pati, Trade-off relations between quantum coherence and measure of many-body localization. *Phys. Rev. B* **111**, 054202 (2025).
58. S. S. Pratapsi, L. Buffoni, and S. Gherardini, Competition of decoherence and quantum speed limits for quantum-gate fidelity in the Jaynes-Cummings model. *Phys. Rev. Res.* **6**, 023296 (2024).
59. L. Tian, A. Govindarajan, P. Parajuli, and K. Cai, Quantum state preparation in Jaynes-Cummings lattices. *J. Phys.: Conf. Ser.* **2912**, 012041 (2024).
60. X. Cao, J. Cui, M. H. Yung, and R.-B. Wu, Robust control of single-qubit gates at the quantum speed limit. *Phys. Rev. A* **110**, 022603 (2024).
61. K. Andrzejewski, Krzysztofand Bolonek-Lasoń and P. Kosiński, Note on the Margolus–Levitin quantum speed limit for arbitrary fidelity. *Quant. Inf. Proc.* **23**, 167 (2024).
62. B. T. Gard, Z. Parrott, K. Jacobs, J. Aumentado, and R. W. Simmonds, Fast high-fidelity quantum nondemolition readout of a superconducting qubit with tunable transverse couplings. *Phys. Rev. Appl.* **21**, 024008 (2024).
63. S. Sun and Y. Zheng, Distinct Bound of the Quantum Speed Limit via the Gauge Invariant Distance. *Phys. Rev. Lett.* **123**, 180403 (2019).
64. T. van der Sar, Z. H. Wang, M. S. Blok, H. Bernien, T. H. Taminiiau, D. M. Toyli, D. A. Lidar, D. D. Awschalom, R. Hanson, and V. V. Dobrovitski, Decoherence-protected quantum gates for a hybrid solid-state spin register. *NATURE* **484**, 82 (2012).
65. J. E. Lang, R. B. Liu, and T. S. Monteiro, Dynamical-Decoupling-Based Quantum Sensing: Floquet Spectroscopy. *Phys. Rev. X* **5**, 041016 (2015).
66. J. Jiang, and Q. Chen, Universal and robust dynamic decoupling controls for zero-field magnetometry by using molecular clock sensors. *Phys. Rev. A* **110**, 043714 (2024).